

# SUMS: synchronous undulator–monochromator scans at Synchrotron Soleil

Manuel Izquierdo,\*<sup>‡</sup> Vincent Hardion, Guillaume Renaud, Lilian Chapuis, Raphael Millet, Florent Langlois, Fabrice Marteau and Christian Chauvet

Synchrotron Soleil, L'Orme de Merisiers, BP 48, St Aubin, 91192 Gif sur Yvette, France.  
E-mail: manuel.izquierdo@xfel.eu

A strategy for performing synchronous undulator–monochromator scans (SUMS) compatible with the control system of Synchrotron Soleil has been developed. The implementation of the acquisition scheme has required the development of an electronic interface between the undulator and the beamline. The characterization of delays and jitters in the synchronous movement of various motor axes has motivated the development of a new electronic synchronization scheme among various axes, including the case when one of the axes is electronically accessible in ‘read-only’ mode. A software prototype has been developed to allow the existing hard continuous software to work in user units. The complete strategy has been implemented and successfully tested at the TEMPO beamline.

© 2012 International Union of Crystallography  
Printed in Singapore – all rights reserved

**Keywords:** X-ray absorption spectroscopy; synchronous scans; hard continuous scans.

## 1. Introduction

The experimental time-resolved investigation of matter with ultra-short pulses, down to the femtosecond time scale, constitutes one of the most active domains in the field of synchrotron radiation, greatly motivated by the emerging free-electron laser facilities where the time variable can be exploited without flux limitations. The scientific interest arises from the aim to precisely understand dynamic processes such as chemical reactions, optically driven phase transitions or magnetization reversal (Chapman *et al.*, 2011; Fausti *et al.*, 2011; Boeglin *et al.*, 2010; Bressler *et al.*, 2009), and also from the possibility of developing new ways to control the properties of materials with potential industrial applications (Gabay & Triscone, 2011).

Since time-resolved experiments require generally at least two sources, one to ‘pump’ the system to the excited state and another to ‘probe’ the evolution of the properties with time, the degree of synchronization between them is the most critical parameter limiting the ultimate time resolution of the experiments. Therefore, synchronization is one of the variables one has to take into account when developing new acquisition strategies at synchrotrons, especially for those beamlines aiming to use the temporal structure of synchrotrons.

Here we address the topic of synchronization strategies applied to a fundamental problem at synchrotrons which is the realisation of ‘gap scans’ with synchronous movement of the undulator and the monochromator. A new gap-scan strategy

developed using Soleil’s control system, SUMS [synchronous (movement and detection) undulator–monochromator scan], will be reported. The development of this type of scan arose from the fact that undulators produce a significant flux only within a narrow bandwidth ( $\Delta E$ )<sup>1</sup> of the fundamental energy  $E$  (selected with a particular gap opening) (Attwood, undated) which is not sufficient to measure absorption edges with X-ray absorption spectroscopy (XAS) at optimal flux. Although solutions for this problem were developed in the late 1990s when insertion devices in undulator mode became the most commonly used photon source at synchrotrons (Rogalev *et al.*, 1998; Pascarelli *et al.*, 1999; Oyanagi *et al.*, 1999; Tanida & Ishii, 2001), the present contribution might be of relevant importance for several reasons: (i) at odds with currently used gap-scan strategies based on a dynamical synchronization between the undulator and monochromator (Rogalev *et al.*, 1998), the presented prototype uses a static synchronization that optimizes the beam time use; (ii) the synchronization between two movement axes has been studied in detail using different schemes, and an electronic solution has been found to synchronize movements down to the nanosecond level; (iii) a general strategy within the specific control system of Synchrotron Soleil has been developed that could be simul-

<sup>1</sup> The bandwidth provided by an undulator is given by  $\Delta E/E \simeq 1/(Nh)$  (Attwood, undated), where  $N$  is the number of magnetic periods and  $h$  is the harmonic of the fundamental gap energy. For example, in the case of the  $L$ -edge of a  $3d$  material like Fe [ $E(L_3) = 706.8$  eV,  $E(L_2) = 719.8$  eV and  $\Delta E = \Delta SO = 13.1$  eV], typical XAS scans are taken in an energy window of 40 eV in order to access the pre- and post-edges necessary to understand the results. The bandwidth of the undulator in this energy range is of the order of 19 eV for the HU44 undulator on the TEMPO beamline with 36 periods. This means scanning a substantial part of the spectrum under non-optimal conditions.

<sup>‡</sup> Currently at European XFEL, Albert Einstein Ring 19, 22761 Hamburg, Germany.

taneously applied to all beamlines at the facility; (iv) the proposed solution is based on industrial components and therefore could be easily implemented elsewhere.

### 2. Preliminary considerations

The optimal implementation of gap scans implies the synchronization of movements between the undulator and the monochromator as well as with the different signal detectors. In this framework the SUMS prototype has made use of the HCS architecture<sup>2</sup> previously developed at Soleil to perform continuous scans with only one movement axis (Langlois *et al.*, 2009).

The hardware system of the HCS uses a commercial CPCI format with industrial I/O counter boards (model PXI 6602 from National Instruments) (<http://www.ni.com/>) and CPCI 2010 ADC boards from ADlink (<http://www.adlinktech.com/>) for the sensor reading coupled to standard industrial boards packaged for the mechanical needs of Soleil (based on the eight-axis GALIL DMC-2182 controller board with a software control unit ‘control box’ and a power converter ‘driver box’) (<http://www.synchrotron-soleil.fr/portal/page/portal/Instrumentation/InformatiqueElectronique/ControleAcquisition>). The software control, developed under the Tango control system (<http://www.tango-controls.org/>), is modular and separates the hardware control from the scan driver. Furthermore, it has the advantage that a preliminary calculation of the trajectories can be directly fed into the electronic control system of the movement axes. This strategy represents a fine optimization over the commonly used dynamical synchronization (Rogalev *et al.*, 1998) since in this case the calculation of trajectories is performed only once (for the first scan) and therefore no time is lost in the verification of relative axes positions during the scan. However, the existing HCS presented several limitations, some of them preventing the implementation of gap scans:

(i) From an electronic point of view, the CPCI-PXI-6602 card requires a 5 V TTL incremental encoder input whereas the TLCC absolute encoders of the undulators provide an SSI output signal not compatible with the HCS hardware.

(ii) The scanning system is only synchronous in detection. This means that when a scan is launched the CPCI-PXI-6602 card starts counting events at a frequency defined by the selected time step independently of whether or not the moving axis has started its movement.

(iii) The movement axes have a ‘delay time’ that affects the performances of the HCS for acquisition times below 50 ms, which indicates the order of magnitude of the underlying delay time.

(iv) The HCS control system accepts only attributes of type ‘position’ for the movement axes, and therefore continuous

scans are performed in encoder units rather than in user units. This reduces the ergonomics of the system and implies the necessity of a post-treatment of measured data to convert them to user units.

In order to develop our optimized SUMS system all these limitations have been addressed. Furthermore, the fact that the electronic control systems of the undulators and the beamlines are independent of each other has been overcome. Since full undulator control is not possible and we can only communicate with them through proxy servers addressing high-level Tango devices, new proxies with attributes ‘position’ and ‘velocity’, compatible with the HCS acquisition system, have been developed.

### 3. Hardware evolutions and synchronization strategies

The hardware modifications for the SUMS have concerned the extraction of a 5 V TTL incremental input signal from the undulator encoder’s gap. This was realised by equipping the standard configuration of one of the four gap encoders [model LT140 from TRelectronic (<http://www.tr-electronic.com/trgroup/TRelectronicenglish.html>)] with an SSI signal output with a precision of 0.2  $\mu\text{m}$  with simultaneous SSI and incremental output signals. Duplication of the encoder output signal is needed to allow normal control of the undulators as well as the possibility to perform the gap scans, and partially motivated by the fact that the precision of the incremental output is half of the SSI precision. Once the incremental signals *A*, *B* and *Z* were available, they were transported to the CPCI-PXI-6602 card at the beamline through a multi-conductor shielded cable of typical length 40 m, and the arrival of a clean signal was successfully tested using an oscilloscope.

Once the signal from the undulator was available at the beamline we concentrated on the synchronization of movements axes. The motivation arises from the observation of anomalous scanning trajectories of the HCS scans for delay times shorter than 50 ms. More concretely, we have systematically noticed that, for acquisition times shorter than this value, the initial position is recorded many times at the beginning of the scan whereas the final position is never reached. This behaviour indicates the existence of a delay time in the movement axis not considered during the development of the HCS system. A series of tests have been performed in order to determine this delay time observed in the HCS scans for one axis scan as well as the jitter uncertainty between the software launch signal and the first TTL pulse indicating the initiation of the axis/axes movement. Tests at the Electronic Control Acquisition (ECA) laboratory and at the TEMPO beamline were performed. The principle of the measurement (depicted in Fig. 1) implies the extraction of the TTL signal from one axis ‘pulse’ (labelled PULS\_i in Fig. 1) generated by the electronic control system control box towards the electronic power converter driver box. A negative TTL pulse commands one motor step movement. One can then measure with this strategy the delay between the first ‘pulse’ signal generation and the first TTL increment coming from one of

<sup>2</sup> HCS stands for ‘hard continuous scan’. This nomenclature has been internally chosen at Soleil to refer to scans in which the motor positions and sensors are synchronously recorded by using electronic schemes. More commonly known under the name of ‘continuous’ or ‘quick-EXAFS’ scans, this generalization was made owing to different classes of experiments in which the technique is used. Furthermore, the word ‘hard’ was introduced to distinguish this type of scan from the ‘scans on-the-fly’ in which motor positions and sensors are recorded with software synchronization.

the encoder's signals (A Encoder in Fig. 1) with the help of an oscilloscope. Two measurements can be made:

(i) MT1: PULS\_1 versus A Encoder1 (and jitter). This measurement was made between a numeric command sent from the control box to the driver box and next to Motor1 (PULS\_1 signal, Fig. 1) and the first step detected on the associated encoder (A Encoder1, Fig. 1). This measurement characterizes delays within a movement axis coming from sources such as the driver box power conversion, motor inertia, mechanical coupling inertia and the encoder response time.

MT2: PULS\_1 versus PULS\_2 jitter. This measurement is made between the PULS\_i signals of different axes and characterizes the jitter coming from different sources: non-deterministic Ethernet layer, control box, embedded software set-up, etc.

The determination of the delay time and jitter is made by launching a persistence loop measurement between two constant positions of the motor axis/axes: P1 to P2. The trajectories of the scans are defined using the scanning graphical user interface (GUI) at Soleil (Salsa) and the loops are generated using the sequencer GUI (Passerelle), the whole software acquisition being developed using the Tango

**Table 1**

Summary results of the delay and jitter characterization with the different synchronization strategies (see text for details).

Synchronization type	MT1 type		MT2 type	
	Delay	Jitter	Delay	Jitter
Software (ECA Laboratory)	5.21 ms	0.09 ms		238 ms
Software (TEMPO)	22.3 ms	1.9 ms		98 ms
SMA (ECA Laboratory)	70.23 ms	10.6 ms	65 ms	10.6 ms
HDM (ECA Laboratory)			245.69 ns <sup>†</sup>	52 ns <sup>†</sup>

<sup>†</sup> Note that the delay and jitter for the HDM electronic strategy are in nanosecond units compared with the results for the other schemes which are in milliseconds.

control system. Initially we characterized the delay and jitter resulting from the software synchronization. Measurements of type MT1 were performed over series of loops of 1000 scans both at the ECA laboratory and at the TEMPO beamline. The results, summarized in Table 1, show that for the laboratory tests the average delay was 5.21 ms with a jitter of 0.09 ms. The obtained value was independent of the axis used and of the encoder/motor ratio. When the same experiments were performed at the TEMPO beamline using one of the beamline slits, we measured a time delay that increased with the integration time with a minimum value of 22.3 ms, which is 4.3

times larger than the average value measured at the laboratory. The measured jitter (1.9 ms) is even more enhanced (a factor of 20) compared with the laboratory results. The software synchronization measurement between two axes, performed with the MT2 measuring scheme, showed a jitter of 238 ms at the laboratory and a smaller value of 98 ms at the beamline.

The jitter value between two axes is too high to consider the software synchronization suitable for the realisation of the SUMS scans. In order to improve the synchronization level we studied two electronic synchronization strategies:

(i) SMA, synchronization of multi-axes scheme, developed at Soleil (Soleil Internal Report). This solution has been included in the embedded software of the control box axes and basically allows the possibility to start motor movements synchronized with an external digital trigger. The trigger in this case will be provided by a PCI-PXI-6602 counting board. When a low state is detected by the control box, it commands a movement on the driver box via a pulse signal where the number of pulses generated on it determines the number of steps the motor will make.

(ii) HDM, hard drive move scheme. The underlying idea is to continuously

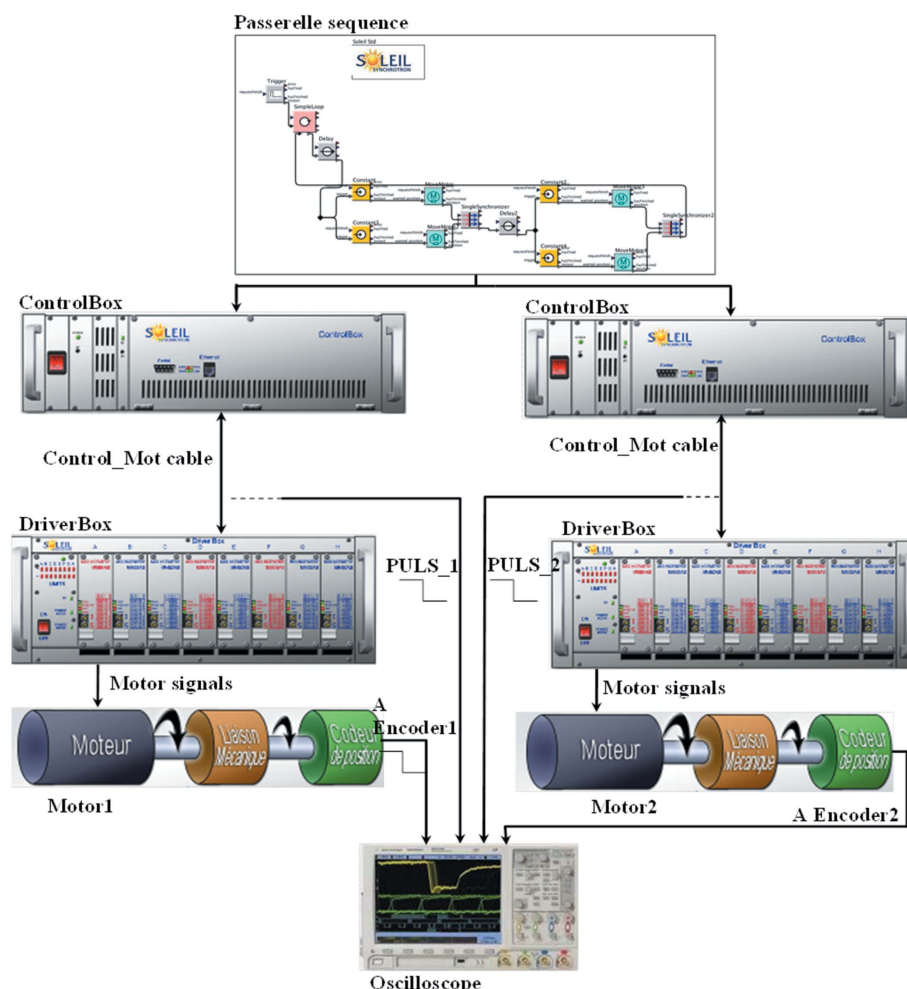


**Figure 1**  
Scheme of the hardware architecture developed to measure delays.

scan the encoder signal of one motor axis (MA1) with a dedicated electronic box and to generate a digital trigger signal when this motor starts moving. The generated trigger will be used as the ‘start move’ input of the control box of the second axis to be moved, thus resulting in master–slave synchronization. The advantage of this configuration is that the master motor axis MA1 is only required to be accessed in ‘read-only’ mode. Furthermore, the continuous scanning of the read-only signal allows the synchronization between the two axes to be customized to better satisfy the experiment requirements.

The results of the characterization of delays and jitter with the electronic strategies have been summarized in Table 1. We can see that the two electronic solutions reduce substantially the jitter in the MT2 measurement between the two motor axes. Furthermore, we have observed that the HDM scheme gives values for the delay and jitter in the nanosecond range, which constitutes by far the best configuration to reduce the jitter down to the nanosecond range. This improves the synchronization level by five orders of magnitude compared with other schemes. Furthermore, since this scheme also allows working with axes in read-only mode, it is also the most suitable for implementing SUMS, since we do not have full control of the undulators.

#### 4. Software developments and implementation of SUMS in user units: TRANSFORMER

In parallel with the electronic hardware modifications and the definition of the best suited synchronization schemes, two software developments were needed. The first one concerns the control of the undulator, which is done through proxy servers owing to the independency of the beamline and undulator control systems. The existing proxies address to high-level Tango devices with the generic name ‘Undulator2-Energy’ that work in user units: energy and polarization. These proxies communicate with low-level Tango devices that calculate the required gap value for a given value of the energy and the polarization. The real command of the undulators is then realised through two attributes, ‘gap’ and ‘gapvelocity’, that cannot be controlled by the HCS system which only understands the ‘position’ and ‘velocity’ attributes. In order to be able to perform SUMS we have created a proxy device that transforms ‘gap’ and ‘gapvelocity’ into ‘position’ and ‘velocity’ attributes. This proxy will perform a bijective unitary transformation of the mentioned attributes and, once created, it should function straightforwardly.

The second and more fundamental development performed has the goal of allowing the realisation of the SUMS in ‘user units’ instead of using the axes ‘position’ and ‘velocity’ units understandable by the CPCI-PXI-6602 card. Although in the first implementation of the HCS system at Soleil the use of common position and velocity attributes was beneficial since it allowed installation over a large number of beamlines, independently of the measurements to be performed, in user operation this fact strongly reduces the performances of the acquisition system. This is because with the present config-

uration users need to configure their scans in axes positions and velocity units, the scanning GUI (Salsa) performs scans into these units and afterwards the user has to transform scans into user units again. This results in a reduction of the ergonomics and functionality of the scanning system, which is not able to transform the measured scans into user units directly. Furthermore, obtaining results in encoder units makes the on-line analysis of data difficult during the experiment.

In order to improve the ergonomics of the acquisition software and to implement it as an evolution of the existing system, the best strategy is to define and test a prototype before the whole acquisition system is changed. We have developed such a prototype that we have named the TRANSFORMER, since its main duty is to transform from user units to position units to launch the scans and to perform the reverse transformation after scans are completed in order to display the scans and store the final results in user units. The TRANSFORMER Tango device has been developed using Groovy [[http://en.wikipedia.org/wiki/Groovy\\_\(programming\\_language\)](http://en.wikipedia.org/wiki/Groovy_(programming_language))]. This choice was made for multiple reasons: (i) this language operates over the Java Virtual Machine installed by default on control computers, (ii) it has a rapid learn-curve by allowing the use of Java language and it is currently used by the ICA team to create Tango devices, (iii) it is also a dynamic language which does not need to be compiled to be executed, which allows the code to be adapted to an unstable process. The actions to be performed by the TRANSFORMER will be the following:

*Energy transformations.* The ‘energy’ devices for both monochromator and undulator directly address to a series of underlying movement axes; therefore they have to be considered as pseudo-motors. The transformation from the energy to axis position can be performed by applying the corresponding formulas.

*Speed transformations.* The scan server computes the velocity of motors to fit the total acquisition time. Owing to the pseudo-motor property of energy devices they do not provide so far the capability to compute velocities. However, these can be easily computed because only one variable is required for each device: the ‘gap’ for the undulator and the deviation angle ‘theta’ for the TEMPO monochromator (which works in constant deviation mode). The acquisition process can take advantage of computing automatically the velocity, average or instantaneous. The latter has the advantage that it is accurate independently of the energy range and step. However, the motor axes controllers should be able to accept a speed trajectory, which has not been available so far. Therefore, for this prototype we have chosen to work with average speeds.

*Sensor transformations.* The Tango device CPCI-PXI-6602 card publishes the results of the corresponding electronic device. This card already transforms the measured pulses into position units ( $^{\circ}$ , rad, mm, etc.). The device commands the card by giving it the current ratio and position from the corresponding motor devices. In the case of sensors, the CPCI-PXI-6602 card counts the number of received pulses, which would be proportional to the intensity of the signal. These pulses are considered to be in user units already.

*Backward transformations.* Once the scan has been measured, the conversion to user units for the monochromator and undulator energies is required.

Once we have defined the required operations we computed a TRANSFORMER class. The function of this class is to create an intermediate software layer of devices between the scan server and the real devices, as depicted in Fig. 2. Six transformer devices are required: two for the monochromator (energy and energy speed), three for the undulator (energy, energy speed and the conversion from undulator ‘gap’ to ‘position’), and one for the CPCI-PXI-6602 card, that hides the real card from the device to the scan server in order to provide the latter with the actuator trajectories in user units. With this new transformer layer the acquisition process has the following structure:

- (i) Salsa computes the velocity, with the initial position, final position and integration time given by the user.
- (ii) The velocity is sent to the scan server together with all the other parameters. When the scan server begins to move the actuators, as in a normal process, the velocity is always set before the next position. Once the energy velocity is set, the device keeps only the value for the next computation of the energy. At this moment the motor velocity is computed.
- (iii) The CPCI-PXI-6602 TRANSFORMER converts the reached position values into energy units for both the undulator and the monochromator and sends the results to the scan server.

### 5. A practical realization of SUMS at the TEMPO beamline

In this section we will present a practical application of the SUMS prototype to the TEMPO beamline, which was the facility used as a template for this project. This beamline has been developed to perform time-resolved experiments in surfaces and interfaces in the energy range from 50 to 1500 eV (Polack *et al.*, 2010). It is equipped with two Apple-II undulators (Marteau *et al.*, 2009, and references therein) with respective periods of 80 mm and 44 mm. The 80 mm-period undulator, although it covers the whole energy range of the beamline, produces an optimal flux with its first harmonic in the 50–600 eV energy range. On the other hand, the HU44 undulator has a period optimized for the 600–1500 eV energy range. For the implementation of the SUMS strategy the HU44 undulator was used. The monochromator works in constant-deviation mode and consists of a system of three variable-groove-depth holographic gratings mounted on a translation stage and coupled to two spherical post-focusing mirrors which produce an image on the exit slits. The change in energy of the monochromator implies a change of the monochromator angle only. Therefore, the realisation of SUMS can be performed with only two movement axes: the undulator gap and the monochromator angle. The implementation tests of the SUMS system have been performed in three steps, described in the following sections.

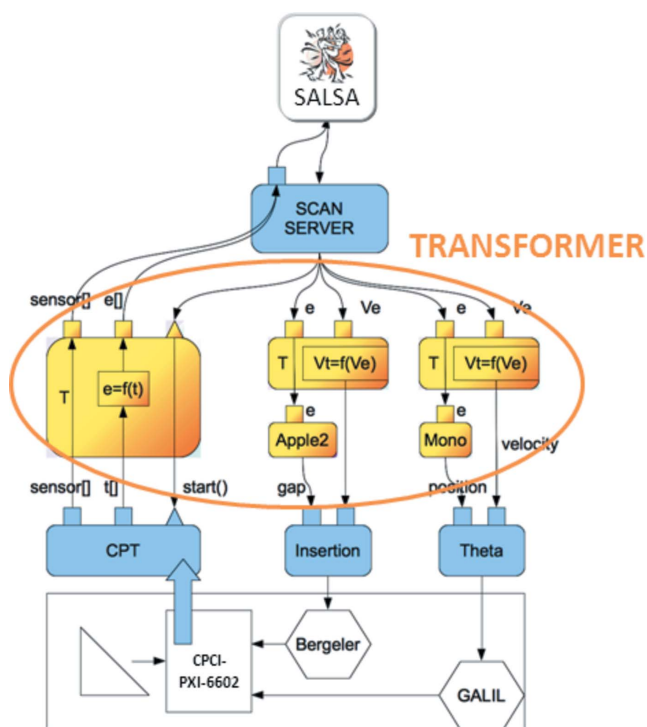


**Figure 2** Acquisition software scheme at Soleil, with the added TRANSFORMER layer for performing scans in user units shown in the ellipse.

#### 5.1. Integration of the undulator in the HCS system

Once the encoder of the HU44 gap was modified to be used within the HCS hardware and the new proxies developed, the performance of the undulator alone was tested. In Fig. 3 we plot a step-by-step scan of the undulator HU44 gap measured using the proxy as ‘actuator’ and the standard undulator gap as ‘detector’ in the Salsa scanning GUI. We can see a perfect one-to-one correspondence between the values in the whole useful gap range of the undulator, *i.e.* between 15.5 and

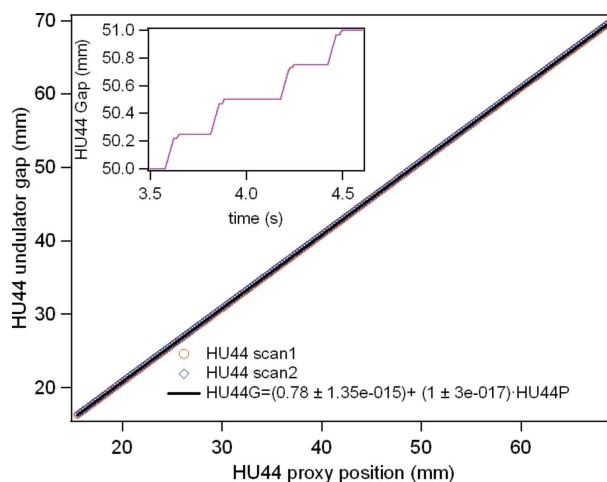


**Figure 3** Step-by-step movement of the HU44 undulator gap using the undulator proxy as actuator. We can see that the movement has the expected ideal slope of 1. The inset shows the movement of the undulator when measured with the CPCI with a time step of  $10^{-4}$  s. The steps reflect the closed-loop movement of the undulator gap.

69 mm. The inset shows a parallel acquisition of the gap movement performed with the CPCI-PXI-6602 at a high frequency, which allows the functioning of the proxy interface to be verified between the undulator axis and the CPCI-PXI-6602 board. This curve has allowed us to detect individual increments of the undulator TTL output signal and also illustrates the underlying closed-loop undulator positioning. The obtained results are very satisfying and indicate already the feasibility of SUMS.

### 5.2. Integration of the TRANSFORMER into the HCS scanning system

In order to test the performances of the TRANSFORMER allowing working in user units we have measured the XAS spectra of a gold grid in total yield mode in the range between 545 and 580 eV. In this energy range Au has, in principle, only one absorption edge ( $N_3 4p_{3/2}$ ) at around 546.3 eV while we have measured a much more complex structure at somewhat higher energies and with a large energy extent. All these features suggest the presence of other atomic species and different oxides. Since our aim is the development of a SUMS prototype, we will concentrate in the following on the different measurement strategies. However, it is worth mentioning that the richness of the spectra was very helpful in the analysis of the different scanning modes. We have performed four types of measurements: (i) a step-by-step (SBS) scan; (ii) an HCS scan in encoder units (named HCS-EU); (iii) an HCS scan with TRANSFORMER for the monochromator (HCS-TRM); (iv) an HCS scan with TRANSFORMER for both undulator and monochromator (HCS-TRUM). The integration time for all scans was 0.1 s, which has been calculated in order to cover the desired energy range in the minimum time possible. This time is limited by the minimum speed of the undulator which is  $10 \mu\text{m s}^{-1}$ . The same value has been chosen in order to be able to perform a quantitative comparison of all scans, although in the first three types the undulator, always in horizontal polarization mode, was kept at a fixed energy of 650 eV (gap = 21.0099 mm). In the last scan type (HCS-TRUM) both undulator and monochromator were moved during the scan with software synchronization only, for which we have measured a jitter of the order of 100 ms. For the SBS scan the drain current was measured in picoamperes while in the other three cases the current signal measured with the picoamperemeter was transformed into pulses for the CPCI-PXI-6602 by means of a current-to-voltage converter. The results,

displayed in Fig. 4, show that qualitatively the four spectra look very similar, with the same features and relative intensity among them. It is also important to notice that the signal-to-noise ratio is as expected, since the integration time is the same in all four cases. The same integration time contrasts with the fact that the scanning time in the case of the SBS scan is 18 times larger compared with the other three cases. This difference is due to the larger time needed for the monochromator to position at the selected energy when moving in a closed-loop mode and indicates that, from the point of view of time optimization, the continuous-scans strategy should be privileged. Furthermore, for continuous scans the sample is less exposed to the photon beam, which implies a reduction of the damage to delicate samples when using the continuous-scanning mode.

To extract more information on the measured scans we have performed a quantitative analysis of the results. A comparison of the SBS scan with the other three was not possible due to the fact that the large scanning time in this case (12 min) would have required normalization with respect to the ring current which was not measured. Concentrating on the other three spectra measured in the same scanning time (40 s) and with the CPCI-PXI-6602, the quantitative analysis was performed by calculating difference spectra. Since the HCS-EU and HCS-TRM spectra should be equivalent except for the fact that the former was determined in encoder units and the latter in user units, two comparisons were made: HCS-TRM with respect to HCS-EU, and HCS-TRUM with respect

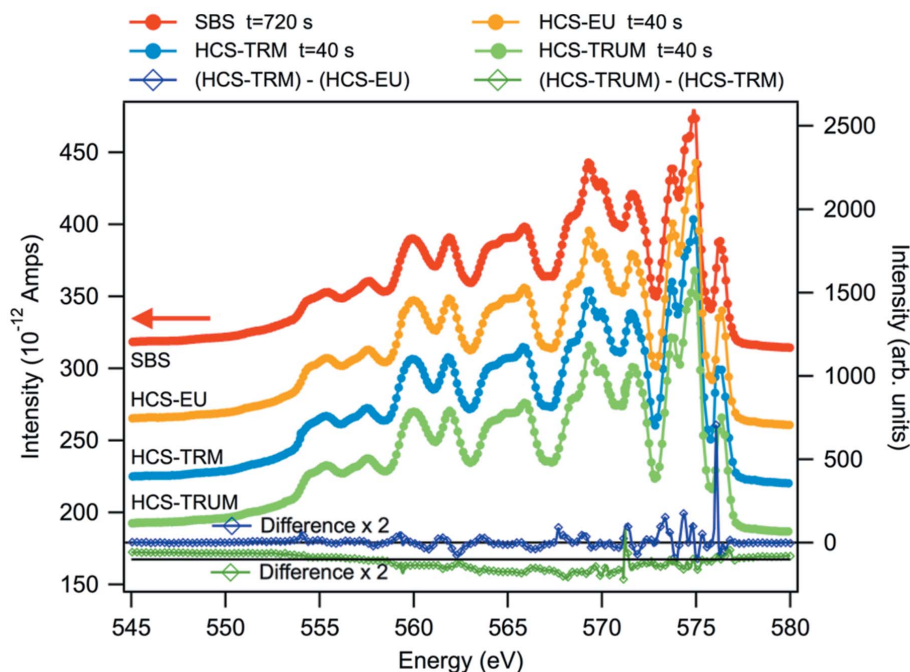


**Figure 4** XAS spectra of a golden grid measured with four different strategies: SBS indicates a step-by-step spectrum measured in picoamperes (left-hand axis). The other three scans, measured in arbitrary units (right-hand axis) correspond to: HCS-EU, existing hard scan in encoder step units; HCS-TRM, HCS scan with the undulator gap fixed and the TRANSFORMER layer applied for the monochromator only; HCS-TRUM, the result obtained for a gap scan with software synchronization between the undulator and the monochromator and the TRANSFORMER layer used to set both undulator and monochromator. Difference spectra (multiplied by 2) used for the quantitative analysis are also displayed (see text for details).

to HCS-EU. The difference spectra are shown in Fig. 4, with the intensity corresponding to the right-hand axis multiplied by two in order to see the differences more clearly. Furthermore, the HCS-TRUM – HCS-EU spectrum has been shifted by 100 arbitrary units of the right-hand axis to better analyse both spectra. We can see that the difference in intensity increases with increasing energy in both cases. This effect is not surprising since as we increase the energy the energy step also increases, the measured points are further apart and therefore errors become larger. We can see this effect from the spike at 576 eV in the HCS-TRM – HCS-EU spectrum which originates from intensity differences at only one point. By comparing the two difference spectra we can observe that differences in the overall spectrum are larger for the HCS-TRUM – HCS-EU spectrum. This result was expected as in this case the undulator is also scanned. Since the difference intensity changes sign with energy, we deduce that when both monochromator and undulator are moved the intensity is flatter, which we aim for with this type of scan. (Note that the measured intensity corresponds to the reference  $I_0$  current that will be used to normalize the intensity at the sample in normal XAS spectra.) Furthermore, we have to keep in mind that the software synchronization between the undulator and monochromator is very poor (jitter 0.1 s) and of the order of the time step. As a consequence, the selected trajectories for undulator and monochromator were not properly synchronized. In a more quantitative analysis of the difference spectra we have performed a statistical analysis of the difference spectra in the range from 545 eV to 575.7 eV to avoid the spike at 576 eV. The average difference value measured for the HCS-TRM – HCS-EU spectrum was 2% compared with the measured intensity, which would correspond to the experimental noise of the system, considering we are comparing single scans. On the other hand, for the HCS-TRUM – HCS-EU spectrum the average difference value is 21% indicating that the movement of the undulator plays an important role in the measured intensity as expected. The overall result from this analysis is that the movement of both undulator and monochromator in user units was correctly performed, which supports the validity of the TRANSFORMER development.

### 5.3. Adding HDM to HCS with TRANSFORMER: SUMS

The final part of the project concerned the integration of the HCS with the electronic synchronization of the undulator and monochromator using the HDM strategy. The test results in this case were performed by using the main experimental station of the TEMPO beamline. We measured the  $2p$  absorption edge on an Fe(001) single crystal in the energy range between 695 and 735 eV for which the HU44 should exhibit an optimal performance.

Measurements were made in linear horizontal polarization in two limiting cases: (i) HCS scan with the transformer at a fixed undulator gap (named HCS-TRM) and (ii) SUM scan with the HDM strategy for the synchronization of the two axes (named SUM). The first result we can extract is that we have

succeeded in implementing the strategy of SUMS with HDM at the beamline. Concentrating on the spectra themselves, they were recorded in 54 s with an integration time of 50 ms. Again the integration time was chosen to optimize the undulator to cover the whole energy range (695–735 eV) at its minimum speed of  $10 \mu\text{m s}^{-1}$ . The results displayed in Fig. 5 for a single scan show the intensity at the sample when measured using the two strategies (Fig. 5a) and the normalized intensity (Fig. 5b). As previously explained, measurements were performed in total yield by measuring the drain current with a pico-ammeter and transforming it into a TTL signal by means of a current-to-voltage converter. We can observe that the signal-to-noise ratio is very good even for a single scan which is not surprising provided we are working with a single crystal. In Fig. 5(a) we can see that the HCS-TRM and SUM spectra show differences in the intensity which increase as the energy increases. This is due to the reduction of the intensity at the high-energy part of the harmonic peak of the undulator. The spectra normalized by the reference ( $I_0$ ) current measured at the gold grid are displayed in Fig. 5(b). The results show that only in the SUMS spectrum does normalization lead to a flat line well above the  $L_2$ -edge, as expected for the XAS spectrum of a bulk single crystal (Stöhr & Siegmann, 2006; Rogalev *et al.*, 1998). This result outlines the importance of performing XAS scans with synchronous movement of the undulator and monochromator in order to always measure at optimal intensity which results in the correct shape of the spectra. Thus, the SUMS strategy represents the most optimized way to perform XAS scans.

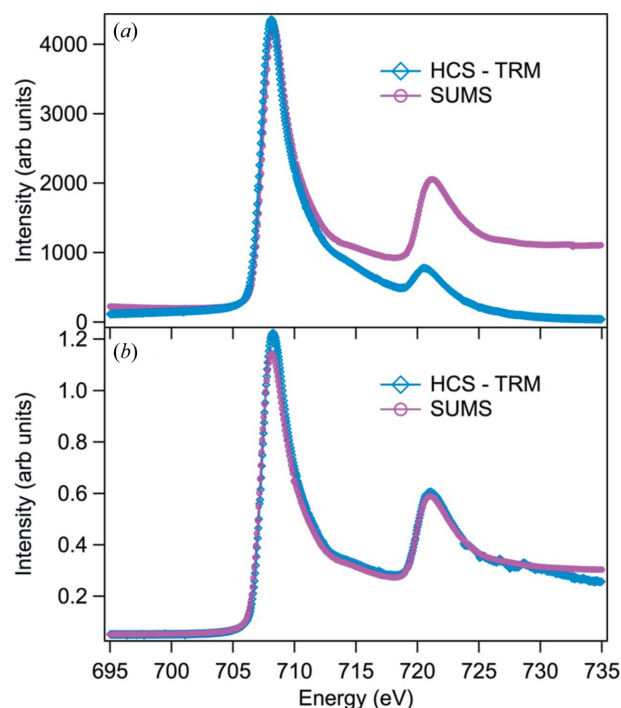


**Figure 5** XAS spectra of the Fe  $L$ -edge measured by using the TRANSFORMER software layer for the monochromator only (labelled HCS-TRM) and in the full SUMS strategy. In panel (a) the intensity at the sample has been represented while in panel (b) the results after normalization by the reference current  $I_0$  are given.

### 6. Conclusions

We have developed a strategy for performing synchronous continuous scans with an undulator and monochromator within the Synchrotron Soleil control system. We have succeeded in interfacing the undulator encoder TLCC system with the CPCI-PXI-6602 card used to perform the hard continuous scans (in read-only mode). We have characterized the delays in the movement axes and demonstrated their importance, as well as those of the jitters, in order to achieve a good synchronization level between movements. Furthermore, we have developed an electronic strategy for performing continuous scans when one of the two axes is accessible in read-only mode, which also minimizes the jitter in the synchronization down to the nanosecond level. This strategy can be applied to multi-axis synchronization and therefore other types of continuous scans could be implemented using it. Furthermore, the nanosecond synchronization level could also be used even for time-resolved experiments on this time scale.

From a software point of view we have developed a prototype to set the scan parameters and to obtain the results in user units. This development will have a positive impact on the preparation of experiments and data treatment since all required conversions will be included in the devices and therefore will be transparent to the users.

The whole strategy and developments have been successfully tested at the TEMPO beamline. Since we have worked within the Soleil GUI scan environment the implementation of this strategy to the other beamlines at Soleil could be performed straightforwardly with small developing cost, which would result in an optimization of resources. Furthermore, the developed strategy could be generalized to synchronize the movement of any selected axes in a beamline. Since all electronics used are based on industrial components, the global strategy could be adopted to develop a general fully synchronized scan system at other facilities.

We would like to acknowledge the support and resources provided by the different group leaders: Marie Emmanuelle Couprie for the GMI (Group Magnetism and Insertions), Pascale Betinelli for the ECA (Electronic Control Acquisition)

and Alain Buteau for the ICA (Informatics Control and Acquisition). We would also like to thank the TEMPO beamline manager F. Sirotti for allowing us to test the final prototype under real conditions. We are also very grateful to Soleil's direction, in particular to Brigitte Gagey (Informatics) and Jean-Marc Filhol (Sources and accelerator and Joint Former Director of Soleil) for their support and to Paul Morin (Scientific Director) for his support and encouragement.

### References

- Attwood, R. (undated). *Soft X-rays & Extreme Ultraviolet Radiation*, <http://www.coe.berkeley.edu/AST/sxreuv>.
- Boeglin, C., Beaurepaire, E., Halté, V., López-Flores, V., Stamm, C., Pontius, N., Dürr, H. A. & Bigot, J.-Y. (2010). *Nature (London)*, **465**, 458–461.
- Bressler, Ch., Milne, C., Pham, V.-T., ElNahhas, A., van der Veen, R. M., Gawelda, W., Johnson, S., Beaud, P., Grolimund, D., Kaiser, M., Borca, C. N., Ingold, G., Abela, R. & Chergui, M. (2009). *Science*, **323**, 489–492.
- Chapman, H. N. *et al.* (2011). *Nature (London)*, **470**, 73–77.
- Fausti, D., Tobey, R. I., Dean, N., Kaiser, S., Dienst, A., Hoffmann, M. C., Pyon, S., Takayama, T., Takagi, H. & Cavalleri, A. (2011). *Science*, **331**, 189–191.
- Gabay, M. & Triscone, J.-M. (2011). *Nat. Photon.* **5**, 447–449.
- Langlois, F., Abeille, G., Renaud, G. & Malik, J. (2009). *Proceedings of the 12th International Conference on Accelerator and Large Experimental Physics Control Systems (ICALEPCS2009)*, Kobe, Japan. WEP054.
- Marteau, F. *et al.* (2009). *Proceedings of the 23rd Particle Accelerator Conference (PAC09)*, Vancouver, BC, Canada. WE5RFP080.
- Oyanagi, H., Ishii, M., Lee, C., Saini, N. L., Kuwahara, Y., Saito, A., Izumi, Y. & Hashimoto, H. (1999). *J. Synchrotron Rad.* **6**, 155–157.
- Pascarelli, S., Neisius, T. & De Panfilis, S. (1999). *J. Synchrotron Rad.* **6**, 1044–1050.
- Polack, F., Silly, M., Chauvet, C., Lagarde, B., Bergeard, N., Izquierdo, M., Chubar, O., Krizmancic, D., Ribbens, M., Duval, J.-P., Basset, C., Kubsy, S. & Sirotti, F. (2010). *AIP Conf. Proc.* **1234**, 185–188.
- Rogalev, A., Gotte, V., Goulon, J., Gauthier, C., Chavanne, J. & Elleaume, P. (1998). *J. Synchrotron Rad.* **5**, 989–991.
- Stöhr, J. & Siegmann, H. C. (2006). *Magnetism: From Fundamentals to Nanoscale Dynamics*, Springer Series in Solid State Science, pp. 152. Heidelberg: Springer.
- Tanida, H. & Ishii, M. (2001). *Nucl. Instrum. Methods Phys. Res. A*, **467–468**, 1564–1567.